Weak antilocalization in high mobility $Ga_xIn_{1-x}As$/InP two-dimensional electron gases with strong spin-orbit coupling

Vitaliy A. Guzenko,[*] Thomas Schäpers, and Hilde Hardtdegen

Institute of Bio- and Nanosystems (IBN-1) and Virtual Institute of Spin Electronics (VISel), Research Centre Jülich, 52425 Jülich, Germany

We have studied the spin-orbit interaction in a high mobility two-dimensional electron gas in a GaInAs/InP heterostructure as a function of an applied gate voltage as well as a function of temperature. Highly sensitive magnetotransport measurements of weak antilocalization as well as measurements of Shubnikov–de Haas oscillations were performed in a wide range of electron sheet concentrations. In our samples, the electron transport takes place in the strong spin precession regime in the whole range of applied gate voltages, which is characterized by the spin precession length being shorter than the elastic mean free path. The magnitude of the Rashba spin-orbit coupling parameter was determined by fitting the experimental curves by a simulated quantum conductance correction according to a model proposed recently by Golub [Phys. Rev. B **71**, 235310 (2005)]. A comparison of the Rashba coupling parameter extracted using this model with the values estimated from the analysis of the beating pattern in the Shubnikov–de Haas oscillations showed a good agreement.

I. INTRODUCTION

Two-dimensional electron gases (2DEGs) with an InAs or high-In-content $Ga_xIn_{1-x}As$ channel layer are very promising candidates for spintronic applications because they show a strong Rashba spin-orbit interaction along with a high electron mobility.[1–3] These properties are essential for the realization of various spintronic devices, e.g., spin field effect transistors,[4,5] spin filters,[6,7] or spin splitters.[8] The strength of the Rashba coupling can be estimated from measurements of Shubnikov–de Haas oscillations by analyzing the characteristic beating pattern.[1–3] However, the latter can also be evoked by inhomogeneities of the sheet carrier concentration[9,10] or due to a slightly occupied second lowest subband;[11] thus, the observance of a beating pattern is not an unambiguous indication of the presence of spin-orbit coupling. On the other hand, the weak localization effect is very sensitive not only to an applied magnetic field but also to spin-orbit coupling. The latter results in a nonmonotonous dependence of the quantum correction to the conductivity on magnetic field. In the case of strong spin-orbit coupling, the quantum correction to the conductivity can even change its sign. The observation of such an effect, also referred to as weak antilocalization (WAL),[12,13] is an unambiguous indication of the presence of spin-orbit interaction. Thus, weak antilocalization measurements open the way for the experimental determination of the contributions to the spin splitting: the linear and cubic Dresselhaus terms,[14] associated with the lack of crystal inversion symmetry, and the Rashba term,[15] resulting from the structural inversion asymmetry. The latter can be controlled by applying an external electric field and is thus, in particular, interesting for spintronic devices.[1,2]

Until recently, only theoretical models describing the weak spin precession regime, also called "diffusion" regime, were available,[16–18] where the elastic mean free path l_{tr} is much shorter than the spin precession length l_{so}.[19,20] However, $l_{tr} \gg l_{so}$ is often found in high mobility 2DEGs comprising a strong spin-orbit interaction. Under such conditions, an experimental observation of the weak antilocalization requires very sensitive magnetotransport measurements, since the width of the WAL peak is often less than 1 mT. From theoretical point of view, extensions of the diffusion models to the case of strong spin precession were only limited to an even narrower range of magnetic fields and thus do not describe the whole WAL curve.[21] Very recently, this problem was solved by the model developed by Golub[22] and later extended by Glazov and Golub,[23] which is valid for both the weak and strong spin precession regimes in 2DEGs.

Taking this into account, we have utilized this model to extract the spin-orbit coupling in high mobility GaInAs/InP samples. By fitting the WAL curves at different gate voltages, we obtained the dependence of the Rashba spin-orbit coupling parameter on the sheet carrier concentration. The results of these measurements were compared with the values extracted from the analysis of the beating pattern of the Shubnikov–de Haas oscillations. We found that despite the fact that the fitting procedure is time consuming due to the numerical complexity, the weak antilocalization measurements might be more advantageous for the determination of the Rashba coupling parameter, since they are also applicable if no beating pattern of the Shubnikov–de Haas oscillations can be observed, e.g., in the case of low mobility.

II. EXPERIMENT

The $Ga_{0.47}In_{0.53}As$/$Ga_{0.23}In_{0.77}As$/InP heterostructure used in our investigation was grown by metal organic vapor phase epitaxy. A 2DEG was formed within the strained $Ga_{0.23}In_{0.77}As$ channel layer. A sketch of the layer sequence is given in Fig. 2 (inset). Conventional 200-μm-wide Hall bar structures with voltage probes separated by 160 μm were defined by optical lithography and reactive ion etching. Subsequently, the AuGe Ohmic contacts were deposited and annealed by rapid temperature processing. Metallic top gates separated from the semiconductor surface by an insulating
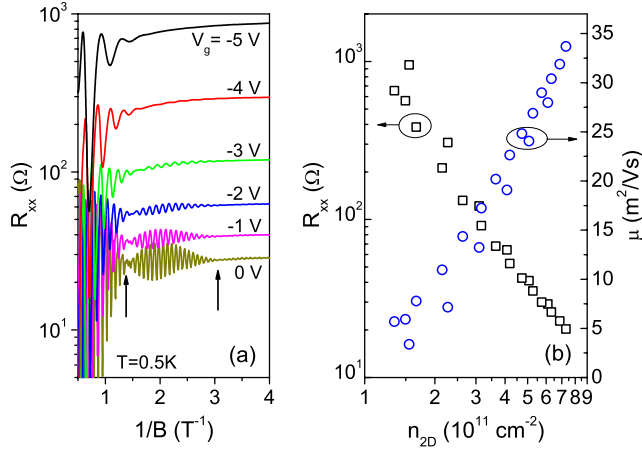
FIG. 1. (Color online) (a) Shubnikov–de Haas oscillations vs inverse magnetic field measured at different gate voltages at a temperature of 0.5 K. The nodes of the beating pattern at zero gate voltage are marked by arrows. The gate voltage was varied from 0 to −5 V in steps of 1 V. (b) Dependence of the zero-field longitudinal resistance and the electron mobility on the sheet carrier concentration. The gate voltage range was [0; −5.9 V].
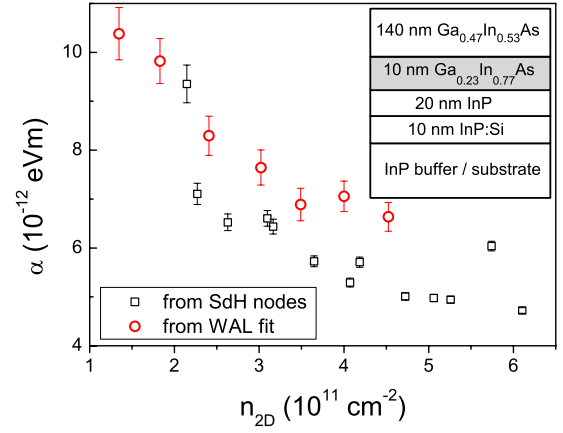

FIG. 2. (Color online) Dependence of the Rashba coupling parameter α on the sheet carrier concentration n_{2D} in our GaInAs/InP 2DEG. A good agreement between the values extracted from the weak antilocalization measurements (circles) and obtained from analysis of the beating pattern of the Shubnikov–de Haas oscillations (squares) is observed. (Inset) A schematic view of the sample cross section. 2DEG is located within the high-In-content GaInAs channel layer.

HSQ layer covered the complete Hall bar structure and allowed us to control the sheet carrier concentration n_{2D} in a wide range, even down to a complete depletion of the 2DEG.

The magnetotransport measurements were performed in a ^{3}He cryostat with a superconducting magnet at temperatures down to 0.4 K utilizing a lock-in technique. Since the WAL effect is strongly temperature dependent, special attention was paid to the electrical power dissipated in the 2DEG. Depending on the changes of the resistance of the sample at different gate voltages, the ac bias current was varied to avoid a heating of the 2DEG. In order to perform weak antilocalization measurements in well-controlled magnetic fields being less than 15 mT, an additionally mounted small superconducting coil was used.

III. DISCUSSION

In order to characterize the 2DEG, Shubnikov–de Haas oscillations were measured in a wide range of gate voltages V_g at 0.5 K. As shown in Fig. 1(a), the magnetoresistance vs inverse magnetic field curves reveal an increase of the oscillation period as well as a change of the beating pattern if the gate voltage is decreased from 0 to −5 V. By performing a fast Fourier transform analysis of the Shubnikov–de Haas oscillations, we determined the corresponding electron sheet densities. No indication of a second subband occupation was found. As can be seen in Fig. 1(b), in the gate voltage range from 0 to −5.9 V, we were able to change the carrier concentration from 7.3×10^{11} to 1.3×10^{11} cm^{-2}. On a long-time scale, i.e., within days, a slight variation of the sheet carrier concentration n_{2D} determined at the same applied gate voltage was observed, possibly due to the presence of the electron states with a long relaxation time at the interface between the semiconductor and the gate insulator. However, the longitudinal resistance R_{xx} as well as the electron mobil-

ity μ remained unique functions of the carrier concentration n_{2D} [see Fig. 1(b)]. As a consequence, we took n_{2D} rather than V_g as a reference for the following analysis of the weak-antilocalization effect.

For our heterostructure, we assumed that the spin-orbit coupling is dominated by the Rashba effect.[3] Indeed, by performing self-consistent band structure calculations and applying the theory presented, e.g., in Ref. 25, the strength of the Dresselhaus and Rashba spin-orbit coupling at several gate voltages was estimated. At zero gate voltage, the ratio between the coupling parameter of the linear Dresselhaus term ($\beta_{calc} = 1.1 \times 10^{-12}$ eV m) and the Rashba term ($\alpha_{calc} = 4.6 \times 10^{-12}$ eV m) is 0.24. With increasing V_g, this ratio becomes even less. The cubic Dresselhaus term, which is strongly dependent on k_F, at zero gate voltage is comparable with the linear one and decreases rapidly with reduced n_{2D}. Thus, in our sample, the spin-orbit coupling is dominated by the Rashba effect. By varying the built-in electrical field and, consequently, the bending of the conductance and valence band profile, the magnitude of the Rashba coupling parameter can be controlled.

In 2DEGs, the Rashba spin-orbit coupling parameter α can be determined from the position of the nodes of the beating pattern in the Shubnikov–de Haas oscillations:[3,24]

$$\alpha = \frac{\hbar e}{2m^* k_F}\left(\frac{1}{B_i} - \frac{1}{B_{i+1}}\right)^{-1},\qquad(1)$$

where k_F is the Fermi wave vector, m^* is the effective electron mass, and B_i is the magnetic field where the ith node is observed. The values of the spin-orbit coupling parameter determined by this method are presented in Fig. 2. As can be seen, α increases with decreasing n_{2D} because of the larger asymmetry of the quantum well profile at more negative gate voltages. As the sheet carrier concentration becomes smaller
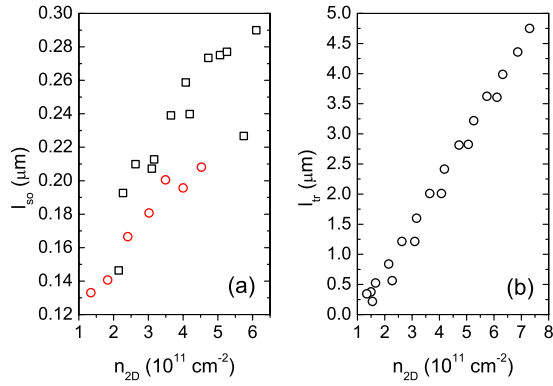
FIG. 3. (Color online) (a) Dependence of the spin precession length l_{so} on the electron concentration n_{2D} extracted from the Shubnikov–de Haas measurements (squares) and from weak antilocalization analysis (circles). (b) The corresponding dependence of the mean free path l_{tr}.

than 2×10^{11} cm^{-2}, the second node [see Fig. 1(a)] cannot be resolved anymore and, consequently, one faces the limitations of the beating pattern analysis technique for the extraction of the Rashba parameter. With the known values of α, the spin precession length can be calculated: $l_{so} = \hbar^2 / \sqrt{2} m^* \alpha$. The values of l_{so} at different electron concentrations are shown in Fig. 3(a). For comparison, the corresponding values of the elastic mean free path l_{tr} are plotted in Fig. 3(b).

We now turn to the measurements of the weak antilocalization effect. As can be seen in Fig. 4 a clear weak antilocalization peak was resolved at $B = 0$ for gate voltages V_g ranging from -3.0 to -5.9 V. Here, the magnitude of the quantum conductance correction was obtained by subtracting the conductance at zero magnetic field from the experimental determined magnetoconductance.[31] Increasing the gate voltage resulted in a strong increase of the sample resistance and simultaneously in a broadening of the WAL peak. Under such conditions, the experimental observation of the WAL effect becomes easier, compared to resolving the beating pattern of the Shubnikov–de Haas oscillations, in particular, at the highest gate voltages. At $V_g \lesssim -2.5$ V, the WAL effect could not be resolved unambiguously.
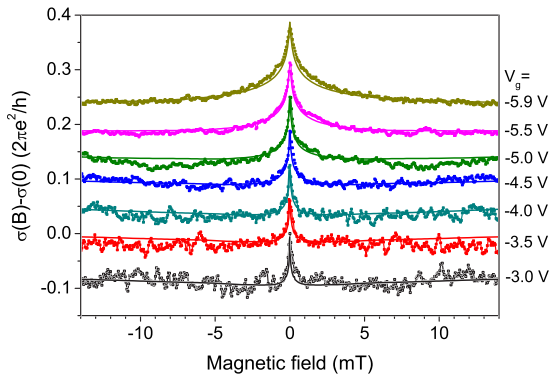

FIG. 4. (Color online) Quantum conductivity correction curves measured at different gate voltages (dots). The curves are vertically shifted for clarity. Solid lines represent the fit by a model in Refs. 22 and 23.

In order to extract the Rashba coupling parameter from the weak antilocalization measurements, the experimental curves were fitted by numerically calculated ones. The choice of the proper model is governed by the transport regime in the sample. In our case, a comparison of the elastic mean free path l_{tr} and the spin relaxation length l_{so} extracted from the findings of the Shubnikov–de Haas oscillations revealed that l_{tr} is larger than l_{so}. This corresponds to the regime of strong spin precession, so that the model in Refs. 22 and 23 has to be applied. It has been shown that the calculated weak antilocalization curves do not differ from each other significantly if the ratio between the coupling parameters β and α is less than approximately 0.6.[23] Since in our case the ratio is less than 0.24, we can readily neglect the Dresselhaus terms in the further analysis. At a given electron concentration, the number of free fitting parameters in the simulations could be reduced from 4 to 2, since the elastic mean free path l_{tr} and the elastic scattering time τ_{tr} were determined directly from the Shubnikov–de Haas measurements and were kept constant during the fitting procedure. The initial value of one of the free parameters, the phase coherence length l_ϕ, was estimated according to Refs. 26–29 and adjusted during the fitting procedure. As can be seen in Fig. 4, a good fit to the experimental curves has been achieved for all gate voltages. The corresponding values of α are shown in Fig. 2.

Knowing the fitting parameters, in particular, the dependence of α on n_{2D}, the corresponding dependence of the spin precession length l_{so} was determined [see Fig. 3(a)]. High electron concentrations, i.e., small negative gate voltages, result in l_{so} which is an order of magnitude shorter than l_{tr}. Applying higher negative gate voltages, i.e., lowering n_{2D}, leads to the rapid shortening of the l_{tr} and, due to the enhancement of the spin-orbit interaction, to the shortening of l_{so}. Despite the decrease of l_{tr} with n_{2D}, l_{tr} is always larger than the corresponding value of l_{so}. Thus, the strong spin precession regime of the electron transport is preserved in the whole range of electron concentrations studied here.

A comparison of the values of α obtained by the analysis of the beating pattern with the ones determined from the WAL measurements reveals a good agreement, although the latter are slightly higher. The origin of this discrepancy is not clear yet. Possibly, the inaccuracy in the determination of the minimum position of the WAL curve caused by the additional contribution of other magnetotransport effects results in an overestimation of the Rashba coupling parameter. As long as the spin-orbit interaction is the only cause of the beatings in the Shubnikov–de Haas oscillations, these two methods are complementary in a certain range of carrier densities. However, at high carrier densities, the observation of WAL is more difficult, since the longitudinal resistance of the sample and consequently the signal-to-noise ratio drop rapidly, whereas the characteristic beating pattern in the Shubnikov–de Haas oscillations can be resolved easily. In contrast, at low electron concentrations, the WAL peak can be easily measured, whereas the position of the nodes cannot be resolved anymore.

Temperature dependent measurements, presented in Fig. 5(a) for a gate voltage of -5.9 V, show a fast suppression of the WAL peak with increasing temperature. Also here, a
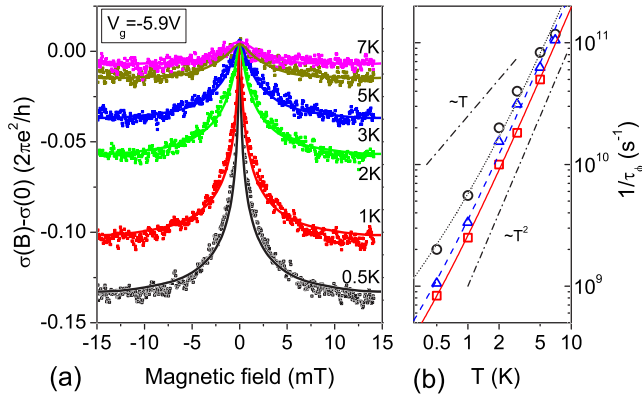
FIG. 5. (Color online) (a) Quantum conductivity correction curves measured at different temperatures with a constant gate voltage (dots). Solid lines represent the fit by a model in Refs. 22 and 23. (b) Temperature dependence of the phase breaking rate $1/\tau_\phi$ extracted from the fits of the WAL curves measured at gate voltages of −5.9 V (circles), −5.5 V (triangles), and −4.5 V (squares). The lines represent the best fit by a function taking into account the T and T^2 dependences of $1/\tau_\phi$ (Ref. 29). The dashed-dotted lines indicate slopes corresponding to T and T^2.

good agreement between the experiment and the model of Glazov and Golub[23] can be readily seen. The only parameter which was varied during the fitting procedure was the phase coherence time τ_ϕ [see Fig. 5(b)].

At low temperatures, the phase breaking rate $1/\tau_\phi$ is essentially determined by electron-electron scattering, which can be divided into two contributions. The first one, being connected to a large-energy-transfer scattering mechanism, leads to a T^2 dependence of $1/\tau_\phi$ and is dominant at $T > \hbar/k_B\tau_{tr}$.[27,28,30] The second contribution, originating from a small-energy-transfer mechanism, depends linearly on T and is most significant at $T < \hbar/k_B\tau_{tr}$.[26,28] As can be seen in Fig. 5(b), the experimental points of the phase breaking rate could be well fitted to a combination of T and T^2 dependences. A comparison with the slopes corresponding to T and T^2 [see Fig. 5(b)] confirms that at higher temperatures ($T > 1$ K), large-energy-transfer scattering with $1/\tau_\phi \propto T^2$ dominates, whereas at lower temperatures, a deviation from a slope proportional to T^2 toward a linear temperature dependence is observed, in particular, at $V_g=−5.9$ V. In fact, at

increasing negative gate voltages, a shift of the crossover temperature $\hbar/k_B\tau_{tr}$ toward larger values is expected, owing to the decrease of τ_{tr} with decreasing electron concentration. In detail, at gate voltages of −5.9, −5.5, and −4.5 V, the crossover temperature was determined to be 5.4, 3.9, and 2.4 K, respectively. In accordance with the theoretical prediction,[26–28,30] an increased scattering rate $1/\tau_\phi$ is found for larger negative gate voltages, i.e., lower n_{2D} and lower τ_{tr}. However, a direct comparison of the values of $1/\tau_\phi$ extracted from the fit to the Golub model[22] with the theoretically determined values[29] reveals that the latter are larger by a factor of about 2. Probably, this discrepancy is connected to uncertainties in the determination of τ_ϕ at large negative gate voltages, which is caused by the weak dependence of the quantum conduction correction on τ_ϕ. As we observed in our calculations, τ_ϕ has a strong effect on the magnitude of the quantum correction at magnetic fields smaller than 0.1 mT, i.e., close to the resolution limit of the experiment. In addition, inaccuracies in the determination of l_{tr} and τ_{tr} from the Shubnikov–de Haas oscillations become more pronounced at large negative gate voltages. In our simulations, we found that these inaccuracies mainly affect the precision in the determination of τ_ϕ.

IV. CONCLUSIONS

In conclusion, we have studied weak antilocalization in a GaInAs/InP 2DEG as a function of electron concentration. Experimental curves were fitted by a universal model which describes both the weak and the strong spin precession regime of the electron transport. Satisfactory fits were achieved in a wide range of gate voltages as well as at different temperatures. We have shown that the dependence of spin-orbit coupling on the gate voltage can be successfully studied in high mobility 2DEGs by analyzing weak-antilocalization measurements. This is a reliable method which is complementary to the beating pattern analysis of the Shubnikov–de Haas oscillations.

ACKNOWLEDGMENTS

*v.guzenko@fz-juelich.de

[1] J. Nitta, T. Akazaki, H. Takayanagi, and T. Enoki, Phys. Rev. Lett. **78**, 1335 (1997).

[2] G. Engels, J. Lange, Th. Schäpers, and H. Lüth, Phys. Rev. B **55**, R1958 (1997).

[3] Th. Schäpers, G. Engels, J. Lange, Th. Klocke, M. Hollfelder, and H. Lüth, J. Appl. Phys. **83**, 4324 (1998).

[4] S. Datta and B. Das, Appl. Phys. Lett. **56**, 665 (1990).

[5] J. Schliemann, J. C. Egues, and D. Loss, Phys. Rev. Lett. **90**, 146801 (2003).

[6] E. N. Bulgakov, K. N. Pichugin, A. F. Sadreev, P. Středa, and P.

Šeba, Phys. Rev. Lett. **83**, 376 (1999).

[7] T. Koga, J. Nitta, H. Takayanagi, and S. Datta, Phys. Rev. Lett. **88**, 126601 (2002).

[8] J. I. Ohe, M. Yamamoto, T. Ohtsuki, and J. Nitta, Phys. Rev. B **72**, 041308(R) (2005).

[9] S. Brosig, K. Ensslin, R. J. Warburton, C. Nguyen, B. Brar, M. Thomas, and H. Kroemer, Phys. Rev. B **60**, R13989 (1999).

[10] N. Thillosen, S. Cabañas, N. Kaluza, V. A. Guzenko, H. Hardtdegen, and Th. Schäpers, Phys. Rev. B **73**, 241311(R) (2006).

[11] D. R. Leadley, R. Fletcher, R. J. Nicholas, F. Tao, C. T. Foxon, and J. J. Harris, Phys. Rev. B **46**, 12439 (1992).

[12] S. Hikami, A. I. Larkin, and Y. Nagaoka, Prog. Theor. Phys. **63**, 707 (1980).

[13] G. Bergmann, Solid State Commun. **42**, 815 (1982).

[14] G. Dresselhaus, Phys. Rev. **100**, 580 (1955).

[15] Y. A. Bychkov and E. I. Rashba, J. Phys. C **17**, 6039 (1984).

[16] S. V. Iordanskii, Yu. B. Lyanda-Geller, and G. E. Pikus, JETP Lett. **60**, 199 (1994).

[17] F. G. Pikus and G. E. Pikus, Phys. Rev. B **51**, 16928 (1995).

[18] W. Knap, C. Skierbiszewski, A. Zduniak, E. Litwin-Staszewska, D. Bertho, F. Kobbi, J. L. Robert, G. E. Pikus, F. G. Pikus, S. V. Iordanskii, V. Mosser, K. Zekentes, and Yu. B. Lyanda-Geller, Phys. Rev. B **53**, 3912 (1996).

[19] T. Koga, J. Nitta, T. Akazaki, and H. Takayanagi, Phys. Rev. Lett. **89**, 046801 (2002).

[20] Ch. Schierholz, R. Kürsten, G. Meier, T. Matsuyama, and U. Merkt, Phys. Status Solidi B **223**, 436 (2002).

[21] J. B. Miller, D. M. Zumbühl, C. M. Marcus, Yu. B. Lyanda-Geller, D. Goldhaber-Gordon, K. Campman, and A. C. Gossard, Phys. Rev. Lett. **90**, 076807 (2003).

[22] L. E. Golub, Phys. Rev. B **71**, 235310 (2005).

[23] M. M. Glazov and L. E. Golub, Semiconductors **40**, 1209 (2006).

[24] B. Das, D. C. Miller, S. Datta, R. Reifenberger, W. P. Hong, P. K. Bhattacharya, J. Singh, and M. Jaffe, Phys. Rev. B **39**, 1411 (1989).

[25] R. Winkler, *Spin-orbit Coupling Effects in Two-dimensional Electron and Hole Systems* (Springer-Verlag, Berlin, 2003).

[26] B. L. Al'tshuler, A. G. Aronov, and D. E. Khmelnitsky, J. Phys. C **15**, 7367 (1982).

[27] G. F. Giuliani and J. J. Quinn, Phys. Rev. B **26**, 4421 (1982).

[28] H. Fukuyama and E. Abrahams, Phys. Rev. B **27**, 5976 (1983).

[29] K. K. Choi, D. C. Tsui, and K. Alavi, Phys. Rev. B **36**, 7751 (1987).

[30] L. Zheng and S. Das Sarma, Phys. Rev. B **53**, 9964 (1996).

[31] This is acceptable because the change of the magnetoconductance due to the Lorentz force, which is a classical effect, is negligible in the range of magnetic field applied here.